particularly accessible because the retina is a thin sheet of tissue that can be readily isolated from the eye. It should also be feasible to use these techniques on brain-slice preparations to study serotonergic neurons in the raphe nuclei.

Note added in proof: Sandell and Masland (*12*) have identified two morphological types of indoleamine-accumulating amacrines in the rabbit retina by injecting Lucifer yellow into cells labeled with 5,7-HT in retina fixed in formaldehyde. Although their type 1 and type 2 cells seem to correspond to the S1 and S2 amacrines of this study, Sandell and Masland reported that the dendritic field diameter of type 1 cells averaged only 376 μm, giving a coverage factor of 16 in the peripheral retina and 50 in the visual streak. In fixed tissue, Lucifer yellow may not diffuse along very thin processes, and the strong fluorescence of the plexus labeled with the 5,7-HT would mask any Lucifer yellow fluorescence in the S1 radial dendrites.

REFERENCES AND NOTES

1. H. G. Baumgarten and A. Björklund, *Annu. Rev. Pharmacol. Toxicol.* **16**, 101 (1976).
2. B. Ehinger, *Vision Res.* **23**, 1281 (1983); N. N. Osborne, *Prog. Retinal Res.* **3**, 61 (1983).
3. B. Ehinger and I. Florén, *Cell Tissue Res.* **175**, 37 (1976); K. Negishi, T. Teranishi, S. Kato, *Neurosci. Lett.* **45**, 27 (1984).
4. To label the serotonin-accumulating neurons, we injected 40 μg of 5,7-HT into the vitreous 60 to 90 minutes before enucleation, or the eyecup was incubated at 37°C in an oxygenated medium [A. Ames and F. B. Nesbett, *J. Neurochem.* **37**, 867 (1981)] containing the 5,7-HT (10 mg/liter, $2.5 \times 10^{-5}M$) for 40 to 60 minutes. Both populations of amacrines accumulated the 5,7-HT in vitro at $10^{-6}M$, as detected by formaldehyde-induced fluorescence.
5. D. I. Vaney, *Proc. R. Soc. London Ser. B* **220**, 501 (1984); M. Tauchi and R. H. Masland, *ibid.* **223**, 101 (1984); D. I. Vaney, *ibid.* **224**, 475 (1985).
6. B. Ehinger and I. Florén, *Exp. Eye Res.* **26**, 1 (1978); N. C. Brecha, C. W. Oyster, E. S. Takahashi, *Invest. Ophthalmol.* **25**, 66 (1984).
7. D. I. Vaney, L. Peichl, B. B. Boycott, *J. Comp. Neurol.* **199**, 373 (1981); R. H. Masland, J. W. Mills, S. A. Hayden, *Proc. R. Soc. London Ser. B* **223**, 79 (1984).
8. H. Wässle, L. Peichl, B. B. Boycott, *Proc. R. Soc. London Ser. B* **212**, 157 (1981); H. Wässle, B. B. Boycott, R.-B. Illing, *ibid.*, p. 177.
9. B. Ehinger and I. Holmgren, *Cell Tissue Res.* **197**, 175 (1979).
10. G. Raviola and E. Raviola, *Am. J. Anat.* **120**, 403 (1967); H. Kolb and E. V. Famiglietti, *Science* **186**, 47 (1974).
11. R. K. Dismukes, *Nature (London)* **269**, 557 (1977); A. Beaudet and L. Descarries, *Neuroscience* **3**, 851 (1978).
12. J. H. Sandell and R. H. Masland, *Soc. Neurosci. Abstr.* **11**, 337 (1985).
13. In the peripheral retina, the cell bodies of the third population of 5,7-HT–accumulating neurons were only faintly labeled and smaller than the S1 and S2 amacrines. The contrast in fluorescence intensity and soma size was less pronounced for cells in the visual streak, but discrimination is a problem only with retinal tissue that has been strongly fixed after incubation periods of 2 hours or longer. Injecting dye into these weakly labeled cells revealed that they are medium-field amacrines that branch in the middle of the inner plexiform layer. When the superfused retina is bleached under ultraviolet excitation, these amacrine cells show a violet fluorescence that contrasts with the blue-yellow fluorescence of the faded S1 and S2 amacrines.

14. I thank P. M. Whitington, A. Hughes, and H. Wässle for comments on the manuscript; P. D. Larsen for animal care; and G. E. Whitington for help with the illustrations. The gift of a microscope camera from the Thomas and Lockyer Charitable Trust is gratefully acknowledged. Supported by National Health and Medical Research Council grants to A. Hughes and D.I.V. The NVRI is an Affiliate Institution of the University of Melbourne.

18 October 1985; accepted 25 February 1986

A Budget for Continental Growth and Denudation

David G. Howell and Richard W. Murray

Oceanic crustal material on a global scale is re-created every 110 million years. From the data presented it is inferred that potential sialic material is formed at a rate of about 1.35 cubic kilometers per year, including hemipelagic volcanic sediments that accumulate at a rate of about 0.05 cubic kilometer per year. It is estimated that the influx of 1.65 cubic kilometers per year of terrigenous and biogenic sediment is deposited on the deep ocean, and this represents continental denudation. Because all this material is brought into a subduction zone, continental accretion rates, which could include all this material, may be as high as 3.0 cubic kilometers per year with a potential net growth for continents of 1.35 cubic kilometers per year.

Although the current volume of continental crust is a relatively well-defined value of 7.6×10^9 km^3 (*1*), the amount and rates of continental growth are controversial (*2–5*). From magnetic lineations, we know that the average age of ocean crust is 55 million years (*6*). Applying this age to the volumes and global budgets of oceanic sediments, ocean crust, volcanic island arcs, seamounts, and circum-Pacific accreted terranes, we can model (i) continental denudation rates, (ii) the growth rate of new crystalline material, specifically volcanic island arcs and seamounts, and (iii) the mix and percentage of rock types available for continental accretion. Comparison of these data to the area, volume, and composition of circum-Pacific terranes provides a qualitative test for the hypothesis of continental growth outlined below. These relations support the contention of some geologists and geochemists (*5*, *7*, *8*) that only a small percentage of sediment is subducted and recycled into the mantle. Thus, most sediment, particularly the clastic-terrigenous component, is accreted to continental margins along with newly formed volcanic rock. In this way, continental material is recycled and the accretion of newly formed volcanic rock results in the net growth of continents.

We used isopach maps (Fig. 1) to determine the total volume of oceanic sediment. Sediment shoreward from the base of the continental rise is not included in our calculations as such material is still part of the continental mass. Major divisional isopachs were plotted on equal area projections at a common scale of 1:10,000,000. The volume between each isopach is described by volume (cubic kilometers) = area (square kilometers) × thickness (kilometers).

Summation of these volumes yields a total sediment volume for each ocean basin (Table 1). This volume is made up of five ingredients: terrigenous debris, volcanic sediment, biogenic silica, biogenic carbonate, and porosity. We did not account for diagenetic products as a separate component.

The determination of the volume of terrigenous plus volcanic material (the nonbiogenic constituents) follows a process that requires as a first step biogenic sedimentation data.

The amount of biogenic silica can be calculated from published estimates of silica accumulation rates based on studies of Deep Sea Drilling Project (DSDP) cores (*9*): silica thickness (kilometers) = average accumulation rate (grams per cubic centimeter per year) × duration of core (years) × 1/density (1/2.30 g/cm^3) × unit conversion (1 km/100,000 cm).

Only 37% of the DSDP sites used in our calculations penetrated the entire thickness of sediment above the basaltic ocean floor. For the remaining 63% of the cores, we assume that the average biogenic silica value continues below the base of the drilled interval down to the basalt floor. The calculated thickness of biogenic silica must also be expanded to account for in situ porosity. The porosity at a depth equal to half the total sediment thickness at the DSDP site

D. G. Howell, U.S. Geological Survey, Menlo Park, CA 94025.
R. W. Murray, U.S. Geological Survey, Menlo Park, and University of California, Berkeley, CA 94720.

(*10*) is used as an intermediate value. This approximation assumes a uniform distribution of biogenic silica. If in situ thickness (kilometers) = silica thickness (kilometers) × [1/(100% porosity)], then per site: silica percentage of total thickness = in situ thickness (kilometers) × 1/total thickness (1/kilometers) × 100.0.

To determine the percentage of biogenic carbonate for each DSDP core, we followed an identical process, using data for porosity (*10*), a density of 2.72 g/cm^3 (*10*), and Sloan's carbonate accumulation rates (*11*). These calculations yield the relative percentage of biogenic material and its inherent porosity at 129 DSDP sites throughout the world ocean basin (Fig. 1). Terrigenous and volcanic sediments, along with pore space, constitute the remaining portion of the thickness.

At each DSDP site, the percentage of terrigenous plus volcanic = 100.0 − silica percentage of total thickness − carbonate percentage of total thickness. This value, plotted at each DSDP site on the equal area maps, is considered indicative of the average nonbiogenic percentage for a given region.

We assume that volcanic sediment compacts similarly to terrigenous sediment; therefore, a separate correction analogous to the expansion of biogenic sediment is not necessary. Because the volcanic sediment volume, derived below, includes only 3% of the total sediment volume (Table 1), this approximation does not significantly affect the final determination of terrigenous volume.

For each isopach area and porosity values from the literature (*12*), terrigenous plus volcanic volume (cubic kilometers) = percentage of terrigenous plus volcanic × (100 − percent porosity) × area (square kilometers) × thickness (kilometers). Summing of these isopach volumes yields a total terrigenous plus volcanic sediment volume per basin.

Finally, for each basin (Table 1), terrigenous volume (cubic kilometers) = terrigenous plus volcanic volume (cubic kilometers) − volcanic volume (cubic kilometers). Or, because we know volcanic accumulation rates (*9*), terrigenous volume (cubic kilometers) = terrigenous plus volcanic volume (cubic kilometers) − average volcanic accumulation rate (grams per square kilometer per year) × [1/density (1/2.2 g/cm^3)] × 1 km/100,000 cm × basin area (square kilometers) × basin age (in years). The terrigenous influx is calculated with division by the basin age (*6*): average terrigenous influx (cubic kilometers per year) = terrigenous volume (cubic kilometers) × 1/age (1/year).

An average accumulation rate per basin for each biogenic sediment type (*9, 11*) is determined from a geographically unbiased selection of DSDP sites with the highest and lowest value per basin disregarded (Table 2).

Similar to the determination of the volcanic volume, biogenic silica influx (cubic kilometers per year) = average silica accumulation rate (grams per square centimeter per year) × 1/density (1/2.30 g/cm^3) × 1 km/100,000 cm × basin area (square kilometers) and, biogenic carbonate influx (cubic kilometers per year) = average carbonate accumulation rate (grams per square centimeter per year) × 1/density (1/2.72 g/cm^3) × 1 km/100,000 cm × basin area (square kilometers). Consequently, for each of the biogenic lithologies (Table 1), sediment volume per basin (cubic kilometers) = influx per basin (cubic kilometers per year) × basin age (year).

In addition to the complications and as-

Table 1. Composition of the volume between the sediment-water interface and the basaltic crust of the five major ocean basins of the world. Total sediment volume = 94.1 × 10^6 km^3.

Ocean basin	Material (×10^6 km^3)					Porosity*	Porosity (%)
	Total volume	Terrigenous	Volcanic	Biogenic $CaCO_3$	Biogenic SiO_2		
North Atlantic	41.2	25.7	0.3	2.8	0.7	11.7	28
South Atlantic	20.2	12.8	0	1.3	0.2	5.7	29
North Pacific	22.4	7.3	1.7	1.7	1.2	10.5	47
South Pacific	17.4	5.1	0.7	3.5	1.8	6.3	36
Indian	40.7	19.4	0.2	6.6	1.1	13.4	33
Total	141.7	70.3	2.9	15.9	5.0	47.6	34

*Calculated as the difference between the total volume and the sum of the terrigenous, volcanic, and biogenic constituents.

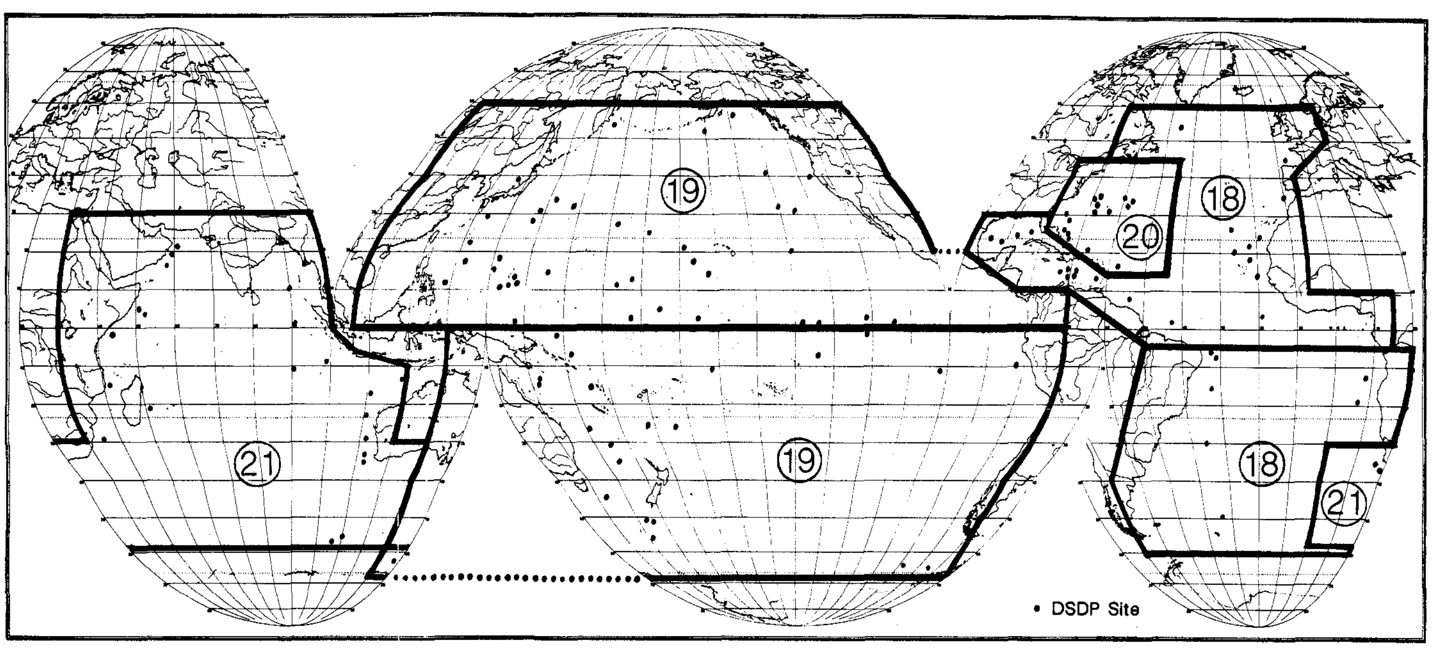

Fig. 1. Goode homolosine equal-area projection of the world oceans showing data sources (*18–21*) and DSDP sites (black dots).

Table 2. Average influxes to the world oceans during the past 55.3 million years. Volcanic and biogenic influxes are calculated directly from the average accumulation rates; terrigenous influx from the world ocean average age of 55.3 million years and the total terrigenous volume from Table 1. Total sediment influx = 1.70 km^3 per year.

Ocean basin	Age (10^6 years)	Average influx (km^3/year)			
		Terrigenous	Volcanic	Biogenic	
				$CaCO_3$	SiO_2
North Atlantic	71.1	0.36	0.004	0.04	0.010
South Atlantic	63.1	0.20	0	0.02	0.003
North Pacific	58.2	0.13	0.030	0.03	0.020
South Pacific	43.9	0.12	0.015	0.08	0.040
Indian	55.4	0.35	0.003	0.12	0.020
Average age	55.3				
Total		1.27	0.052	0.29	0.093

sumptions discussed above, other approximations are necessary to calculate world sediment influxes and volumes.

1) The published values of silica accumulation rates (*9*) are stated to have a possible 7% error. Results from smear slide analysis are consistently 13 percentage points higher than rates found at the same DSDP site when a normative calculation technique is needed (*9, 13*). As the normative technique values are not published for a large number of drilling locations, the discrepancy was accommodated by subtracting 13 points from each final silica percentage at the DSDP locations used in this study.

2) The accumulation rates are available for DSDP holes only. The average area represented by each of the 129 sites is approximately 1.2×10^6 km^2 with the South Pacific and southern Indian oceans most notably lacking data points (Fig. 1). However, there is little sediment in the South Pacific (averaging less than 150 m thick) and most of the Indian Ocean sediment is held in the Indus and Bengal fan systems. Although the data are sparse in some regions of the world, the overall coverage appears to be adequate to generate meaningful values for composition of the sedimentary cover in the deep sea.

3) The arctic basins were not included primarily because of the paucity of accurate data on sediment thickness and composition beneath the ice cap. Yet, major high latitude river systems draining into the Arctic Ocean contribute only 1.3% of the total worldwide sediment discharge (*14*). Furthermore, because of the wide continental margins of the Siberian and Scandinavian Arctic, it is probable that only a small fraction of this 1.3% ever reaches the deep ocean basins. As such, the omission of the Arctic basins does not critically affect our data base.

What is the continental growth potential? The 1.27 km^3 per year total terrigenous influx to the world ocean basins (Table 2) equals 21% of the total suspended and bedload sediment discharge of all rivers (*14*); the remaining 79% is deposited on the submerged parts of continents. We assume the dissolved load component of river discharge is manifest either in the biogenic sediments or possibly as a minor diagenetic component. The total terrigenous and biogenic discharge flux (1.65 km^3/year) to the ocean floor represents an effective rate of continental denudation. The amount of crustal material added to continents must surpass this denudation if continental growth is to be realized.

Table 3. Areal distribution of accreted terranes of the circum-Pacific during the last 200 million years. Continental fragments are considered as separate from remaining lithologies as they represent no net addition to the world crustal volume.

Depositional and tectonic environments of dominant lithologies	Area of accretion (%)	
Oceanic volcanic island arcs	62.6	
Volcanic arcs with probable Precambrian basement	2.3	
Subtotal		64.9
Oceanic rocks mixed with terrigenous sediments	16.5	
Oceanic rocks, crust, seamounts, hot spot tracks	3.4	
Subtotal		19.9
Continental fragments with Precambrian basement	10.5	
Composite terranes	4.7	
Subtotal		15.2
Total		100.0

Table 4. Relative volumes of material available for accretion in the Pacific basins and the entire world oceans. The high volume of island arc material in the Pacific is due to the many convergent plate margins that characterize the region's "ring of fire."

Basin components	Pacific basins (%)	World ocean basins
Volcanic arcs	51.7	36.6
Terrigenous sediments	18.1	42.3
Seamounts	14.7	6.7
Biogenic sediments	12.0	12.7
Volcanic sediments	3.5	1.7
Total	100.0	100.0

Some data suggest a yearly growth of seamounts at a rate of 0.2 km^3 per year and subduction related volcanic edifices at approximately 1.1 km^3 per year (*1*); we estimate the yearly influx of terrigenous, biogenic, and volcanic material to the ocean is 1.70 km^3 per year (Table 2). Until more is known about how much of the material entering a subduction zone actually progresses into the mantle, we cannot compute actual rates of continent growth. Nonetheless, the above figures suggest that 3.00 km^3 per year of material is available for continental crustal accretion. This available material minus the denudation estimate of 1.65 km^3 per year equals a maximum potential for continental growth of 1.35 km^3 per year (approximately 43 m^3 per second).

The compilation of circum-Pacific tectonostratigraphic terranes (*15*) offers a qualitative test to assess the rates and relative percentages of oceanic material accreted to continents. These terranes are fault-bounded crustal bodies that form the building blocks of orogenic systems along the margins of continents (*16*). The accretion and rearrangement of terranes causes continents to grow and change shape. The circum-Pacific terranes are characterized either by the basement rock type (for example, volcanic arcs) or principal rock type (for example, oceanic rock with terrigenous sediment). Because the crustal depth of each terrane is not known, we can only calculate the relative percentages based on the areal distribution (Table 3). This comparison assumes that the area of outcrop of terranes is representative of and seemingly proportional to the volumes of terranes. Clearly, deep crustal data are needed to test this assumption. We restrict our analysis to terranes accreted since the breakup of Pangaea approximately 200 million years ago.

The comparison of what has been accreted (Table 3) to what is currently available for accretion within the Pacific Ocean or the global oceans overall (Table 4) strengthens the argument for continental growth. Though a one-to-one correlation is not evident, the two are remarkably similar, but for several notable exceptions. Seamounts in the Pacific account for 14.7% (within all the modern ocean basins 6.7%), both values are larger than the 3.4% found in the terrane collage. The same is true for biogenic (pelagic) sediment where it represents approximately 12% of potentially accretable volume, but is too small a percentage to depict on the circum-Pacific terrane map. These relations may indicate physical properties that render seamounts and pelagic sediment to be more susceptible to subduction, continental underplating, recycling into the mantle, or both.

The percentages of terrigenous sediment and volcanic debris in the Pacific Ocean and in the circum-Pacific terranes are rough equivalents lending credence to the hypothesis that continents are growing. On a global scale, terrigenous debris accounts for a bigger percentage, up to 42%. This reflects the large accumulation of sediment along trailing margins (Indian and Atlantic oceans). Even though this material is destined for accretion following a Wilson cycle-like ocean closure, the margin of Panthalassa must not have included major portions of long-lived passive plate regimes.

The total area of the circum-Pacific consisting of terranes accreted since 200 million years ago is approximately 33×10^6 km^2 (*15*). Assuming an average crustal thickness of 20 km, one calculates an accretionary rate of 3.3 km^3 per year since the breakup of Pangaea. This value is too large for a continental growth estimate because recycled sediment as well as terranes older than 200 million years are included in the volume calculation. Not until we know the thickness of all terranes younger than 200 million years and can determine the amount of material that is subducted into the mantle will we be able to precisely calculate the rate of continental growth; at this point, the estimates of 3.0 km^3 per year for accretion and 1.35 km^3 per year for continental growth provide a framework for discussion.

REFERENCES AND NOTES

1. A. Reymer and G. Schubert, *Tectonics* **3**, 63 (1984).
2. C. J. Allegre, *Tectonophysics* **81**, 109 (1982).
3. S. M. McLennan and S. R. Taylor, *J. Geol.* **90**, 347 (1982).
4. R. K. O'Nions *et al.*, *J. Geophys. Res.* **84**, 6091 (1979).
5. J. Veizer and S. L. Jansen, *J. Geol.* **87**, 341 (1979).
6. J. G. Sclater *et al.*, *J. Geophys. Res.* **86**, 11535 (1981).
7. D. E. Karig and R. W. Kay, *Philos. Trans. R. Soc. London Ser. A* **301**, 233 (1981).
8. R. W. Kay, *J. Geol.* **88**, 497 (1980).
9. K. J. Miskell *et al.*, *Bull. Am. Assoc. Pet. Geol.* **69**, 996 (1985).
10. E. L. Hamilton, *J. Sediment. Petrol.* **46**, 280 (1976).
11. J. Sloan, unpublished data.
12. B. Baldwin and C. O. Butler, *Bull. Am. Assoc. Pet. Geol.* **69**, 622 (1985).
13. M. Leinen, *Geochim. Cosmochim. Acta* **41**, 671 (1977).
14. J. D. Milliman and R. H. Meade, *J. Geol.* **91**, 1 (1983).
15. D. G. Howell *et al.*, American Association of Petroleum Geologists, Tulsa, OK, (1985), scale 1:17000000.
16. E. R. Schermer, D. G. Howell, D. L. Jones, *Annu. Rev. Earth Planet. Sci.* **12**, 107 (1984).
17. J. C. Moore, *Geology* **3**, 350 (1975).
18. K. O. Emery and E. Uchupi, *The Geology of the Atlantic Ocean* (Springer-Verlag, New York, 1984).
19. W. J. Ludwig and R. E Houtz, American Association for Petroleum Geologists, Tulsa, OK, (1979), scale 1:15000000.
20. B. E. Tucholke *et al.*, *Bull. Am. Assoc. Pet. Geol.* **66**, 1384 (1982).
21. G. B. Udintsev *et al.*, Eds., *Geological-Geophysical Atlas of the Indian Ocean* (Pergamon, New York, 1975).

22. We thank G. McHendrie and S. Fox for their computer assistance and T. Wiley for helpful discussion. We are grateful to J. Sloan for allowing use of his unpublished carbonate accumulation rates (supported by NSF grant OCE8409369). Suggestions by R. Stanley and D. Rubin improved the clarity of early drafts. This work was partially funded by USGS/DOE interagency agreement DE-AI21-83-MC20422.

27 January 1986; accepted 8 May 1986

The 1985 Central Chile Earthquake: A Repeat of Previous Great Earthquakes in the Region?

D. Comte, A. Eisenberg, E. Lorca, M. Pardo, L. Ponce, R. Saragoni, S. K. Singh, G. Suárez

A great earthquake (surface-wave magnitude, 7.8) occurred along the coast of central Chile on 3 March 1985, causing heavy damage to coastal towns. Intense foreshock activity near the epicenter of the main shock occurred for 11 days before the earthquake. The aftershocks of the 1985 earthquake define a rupture area of 170 by 110 square kilometers. The earthquake was forecast on the basis of the nearly constant repeat time (83 ± 9 years) of great earthquakes in this region. An analysis of previous earthquakes suggests that the rupture lengths of great shocks in the region vary by a factor of about 3. The nearly constant repeat time and variable rupture lengths cannot be reconciled with time- or slip-predictable models of earthquake recurrence. The great earthquakes in the region seem to involve a variable rupture mode and yet, for unknown reasons, remain periodic. Historical data suggest that the region south of the 1985 rupture zone should now be considered a gap of high seismic potential that may rupture in a great earthquake in the next few tens of years.

Central Chile, between 32° and 35°S, has been the site of great earthquakes in 1575, 1647, 1730, 1822, and 1906. This sequence gives a remarkably constant return period of 83 ± 9 (mean ± SD) years for great shocks in the region. On the basis of this sequence and the validity of time- and slip-predictable models of earthquake recurrence, the region had been identified as a gap of high seismic potential, and a great earthquake had been forecast for this decade (*1–3*).

On 3 March 1985 (22:46:56.8 GMT) the central Chilean coast was struck by a great earthquake (surface-wave magnitude, $M_s = 7.8$), which caused serious damage to the coastal towns from Quintero in the north to Matanza in the south (distance of about 150 km) as well as to many inland towns and cities including Santiago (Fig. 1) (*4*). The earthquake appears to have fulfilled the forecast if we ignore an earthquake in 1971 ($M_s = 7.9$) that broke the northern one-third of the estimated rupture length of the 1906 shock.

To explain the periodic sequence of the great shocks, the currently popular time- and slip-predictable models of earthquake recurrence (*5*, *6*) require nearly constant rupture lengths. Our analysis of the data, however, shows that the great earthquakes in the region are not similar to each other; their rupture lengths vary by a factor of about 3. The great shocks of central Chile demonstrate that our understanding of the earthquake generation process is still very rudimentary and that there may not be a single universal model valid for all seismic regions of the world.

The main shock of 3 March 1985 was preceded by intense foreshock activity, which began with an event of bodywave magnitude (m_b) of 4.7 on 21 February at 18:53:08.5 GMT. The frequency of the foreshocks caused great alarm in Valparaíso (*7*). In the next 11 days the permanent central Chilean network recorded 360 earthquakes with coda magnitudes (M_c) of >3.0 (*8*) (Fig. 1). On 2 March 1985 the water wells serving a community near the coast of

D. Comte, A. Eisenberg, M. Pardo, Departamento de Geología y Geofísica, Universidad de Chile, Santiago, Chile.
E. Lorca, Instituto Hidrográfico de la Armada, Valparaíso, Chile.
L. Ponce and G. Suárez, Instituto de Geofísica, Ciudad Universitaria, Universidad Nacional Autónoma de México, 04510 México, DF.
R. Saragoni, Departamento de Ingeniería, Civil, Universidad de Chile, Santiago, Chile.
S. K. Singh, Instituto de Geofísica and Instituto de Ingeniería, Ciudad Universitaria, Universidad Nacional Autónoma de México, 04510 México, DF.